Mon. Not. R. Astron. Soc. **286,** 85–96 (1997)

Mid- and far-infrared polarimetric studies of the core of OMC-1: the inner field configuration

David K. Aitken,[1] Craig H. Smith,[2] Toby J. T. Moore,[2] Patrick F. Roche,[3] Takuya Fujiyoshi[2] and Christopher M. Wright[4]

[1]*Division of Physical Sciences, University of Hertfordshire, College Lane, Hatfield, Herts AL10 9AB*
[2]*School of Physics, University College, ADFA, UNSW, Canberra, ACT 2600, Australia*
[3]*Department of Astrophysics, Oxford University, Keble Road, Oxford OX1 3RH*
[4]*Max-Planck-Institut für extraterrestrische Physik, Postfach 1603, D-85740, Garching, Germany*

Accepted 1996 October 8. Received 1996 September 27; in original form 1996 June 24

ABSTRACT

We present imaging polarimetry of the central 30 arcsec of OMC-1 at 12.5 and 17 μm with arcsecond resolution, together with complementary spectropolarimetry in the ranges 8–13 and 16–22 μm at selected positions, and polarimetry at 800 μm over an approximately 1-arcmin field.

The polarization is due to the dichroism of aligned grains in emission in the far-infrared, and predominantly due to absorption in the mid-infrared. The images reveal large variations of polarization fraction and position angle in BNKL, the central region, and these can explain the low fractional polarization observed when this region is unresolved, as in the far-infrared.

The mid-infrared polarization indicates that a substantial component of magnetic field is aligned with the plane of the disc-like structures inferred from millimetre-wave studies, and suggests the presence of a toroidal field within the disc.

Key words: polarization – stars: formation – dust, extinction – ISM: individual: OMC-1 – ISM: magnetic fields – infrared: ISM: continuum.

1 INTRODUCTION

The giant molecular cloud OMC-1 has been studied extensively over a wide wavelength range (e.g. Genzel & Stutzki 1989 for a review), and its relative proximity and high luminosity have allowed more detailed study of it than of any other region of ongoing massive star formation.

In this investigation we are principally concerned with the magnetic field distribution in the mid-infrared luminous core region of OMC-1, generally held to be excited by the infrared source Irc2, or a source in its close proximity, and the relationship of these fields to the almost uniform field, revealed by far-infrared studies (Gonatas et al. 1990; Leach et al. 1991; Hildebrand et al. 1995), which seems to pervade most of OMC-1. In these studies OMC-1 appears as an elongated ridge running roughly north-north-east, the polarization of which, here due to dichroic emission from aligned grains, indicates a magnetic field essentially normal to the ridge. The polarizations observed through the far-infrared, from 100 μm to 1.3 mm, are generally large and of order 3–6 per cent except in the very central region, close to the Becklin–Neugebauer object (BN) and Irc2, where the polarization reaches a minimum $\lesssim 2$ per cent. Gonatas et al. (1990) considered that this might be attributed to a reduction in alignment efficiency owing to changes in grain shape and composition; there was no indication that density or temperature differences affected alignment. Leach et al. (1991) considered as well the possibility that field complexity in the central region may reduce the polarization. All these far-infrared observations were of low spatial resolution with beam diameters > 15 arcsec.

Large 10-μm polarization of the BN object was first observed by Dyck et al. (1973), and subsequent studies of its spectral profile were reported by Dyck & Lonsdale (1981) which, because of the slight shift of polarization maximum with respect to the extinction maximum, unambiguously established that the polarization was due to dichroic absorption by aligned grains (Martin 1975). For the same wavelength region Aitken et al. (1985) presented results which showed large variations of polarization and position angle within several arcseconds of Irc2 with a strong tendency for the *E* vectors to point towards Irc2. Because of this associa-

tion Aitken et al. (1985) attributed the alignment mechanism to the intrinsic angular momentum of photons (Harwit 1970) in the outwardly directed radiation field from Irc2.

At this point it is worth emphasizing that, although the alighment mechanism is still not well established (rather, there appear to be a number of possibilities, and different mechanisms may operate in different environments), the average orientation of a non-isotropic distribution of grain spins will be determined by the ambient magnetic field (e.g. Dolginov & Mytrophanov 1976; Lazarian 1994) irrespective of the mechanism that produces the anisotropy. This is because the magnetic moment induced in spinning grains through the Barnett effect will ensure that individual grains precess about the ambient field with a precession period much shorter than any of the processes involved in disturbing the isotropy of the grain spin distribution. Thus, while the intrinsic angular momentum of photons could still be a contributing factor to grain alignment near Irc2, the variations in position angle observed must denote large field variations within the mid-infrared source, the Becklin–Neugebauer–Kleinmann–Low nebula (BNKL), with a tendency for the projected field direction to be towards Irc2.

The polarization of the S(1) 2.12-μm molecular hydrogen line, attributed to dichroic absorption (Hough et al. 1986), in the inner region of Orion also showed field variations close to Irc2, and this was the first evidence of such field variations to be published. Further work (Burton et al. 1991; Chrysostomou et al. 1994) has repeated and confirmed these observations with more complete coverage and higher spatial resolution, and models have been developed of the field configuration within the central regions of Orion.

The molecular hydrogen line studies are dependent on the distribution and location along the line of sight of the excited H_2, and it is not clear to what extent there may be contamination from scattering, which clearly dominates the polarization at greater distances from Irc2. Additionally, the S(1) polarization probably arises from relatively small optical depths within the cloud since, as pointed out by Burton et al. (1991), its polarization is much less than the polarization of the *K*-band continuum radiation close to the BN object.

The thermal emission from dust in the mid-infrared is more concentrated about the central regions than the S(1) radiation, probes deeper into the cloud than this or the near-infrared continuum, and is negligibly affected by contamination from scattered light. Thus studies in the thermal infrared can augment the knowledge of the field distribution revealed by the near-infrared observation; we present imaging polarimetry at 12.5 and 17 μm of the inner 30 arcsec of OMC-1, the BNKL complex, at a spatial resolution of 1 arcsec.

2 OBSERVATIONS

Polarimetric images were obtained at $\lambda = 12.5$ μm ($\Delta\lambda = 1$ μm) at the 3.9-m Anglo-Australian Telescope (AAT) in 1993 July and at $\lambda = 17$ μm ($\Delta\lambda = 2$ μm) at the 3.8-m United Kingdom Infrared Telescope (UKIRT) in 1995 January using our mid-infrared imaging polarimeter NIMPOL/MIRAS. This instrument, based on an Amber Engineering 128 × 128 DRO Si:Ga array, provided adequately oversampled diffraction-limited images on both telescopes with a pixel size of 0.25 arcsec and a field of view of 32 × 32 arcsec^2.

A fixed analyser consisting of a wire grid on a KRS-5 substrate was mounted on the liquid helium cooled working surface near a Lyot stop; the incoming plane of polarization was rotated by a warm CdS (10-μm region) or CdSe (20-μm region) $\lambda/2$ waveplate mounted on the telescope axis. Images were obtained with waveplate rotations of 0°, 22°.5, 45° and 67°.5 from an arbitrary zero. From this set of four images, further images corresponding to Stokes *I*, *Q* and *U* were derived. Position angle calibration was taken from the known value of 118° for BN (e.g. Aitken et al. 1985) and the polarization corrected for the known waveplate efficiencies at 12.5 and 17 μm. The instrumental polarization is measured to be < 0.5 per cent, determined from observations of unpolarized standard stars. Details of the instrument design, etc., are presented by Smith, Aitken & Moore (1994).

Complementary to this work have been spectropolarimetric observations in the ranges 8–13 and 16–22 μm using the UCL cooled grating spectropolarimeter on UKIRT in 1991 and 1992, which extend those reported by Aitken et al. (1985), and 800-μm observations with the common-user bolometer UKT14 and the Aberdeen polarimeter on the 15-m James Clerk Maxwell Telescope (JCMT). The 800-μm polarization measurements were made at several positions in and around the Orion core, with a 14-arcsec circular beam, on 1992 November 23–25. Standard chopping and nodding techniques were used with a beam displacement of 90 arcsec in azimuth, and with the waveplate driven in steps of 22°.5. The instrumental polarization of 0.9 per cent at a position angle of 178°, which is largely introduced by the mesh windblind, was determined through measurements of Mars, Saturn and Jupiter which are assumed to be unpolarized. Corrections appropriate to the elevation of the source for each measurement were applied to the Stokes parameters.

3 RESULTS AND DISCUSSION

Fig. 1(a) shows polarization vectors superimposed on the 12.5-μm surface brightness contours. The surface brightness has been smoothed to a 0.8 arcsec FWHM Gaussian and the contours truncated at ≃25 per cent of the BN object peak. The polarization data have been similarly smoothed to 1.5 arcsec FWHM and presented every third row and column of the array. The coordinate offsets in Fig. 1 are in arcsec from the position of BN. The same offset scale (from BN) is also used for Figs 2, 5 and 7 (see later).

The flux in the 12.5-μm image is concentrated mainly in the discrete sources Irc2, Irc3, Irc4, Irc7 and especially the BN object; there are clear, large differences in polarization between these regions. Elsewhere the diffuse surface brightness is low and here the polarimetry is poorly defined on account of the low signal-to-noise ratio. Irc2 is complex, as revealed by observations at 3.8 μm of Dougados et al. (1993) where four distinct components are seen. Detail from the 12.5-μm image in the region of Irc2 and Irc7 is shown in Fig. 1(b), where the smoothing Gaussian is 0.4-arcsec FWHM and more closely spaced contours show the finer structure. This complements the 8.7-μm image of Gezari & Backman (1993) where much the same features are seen, including

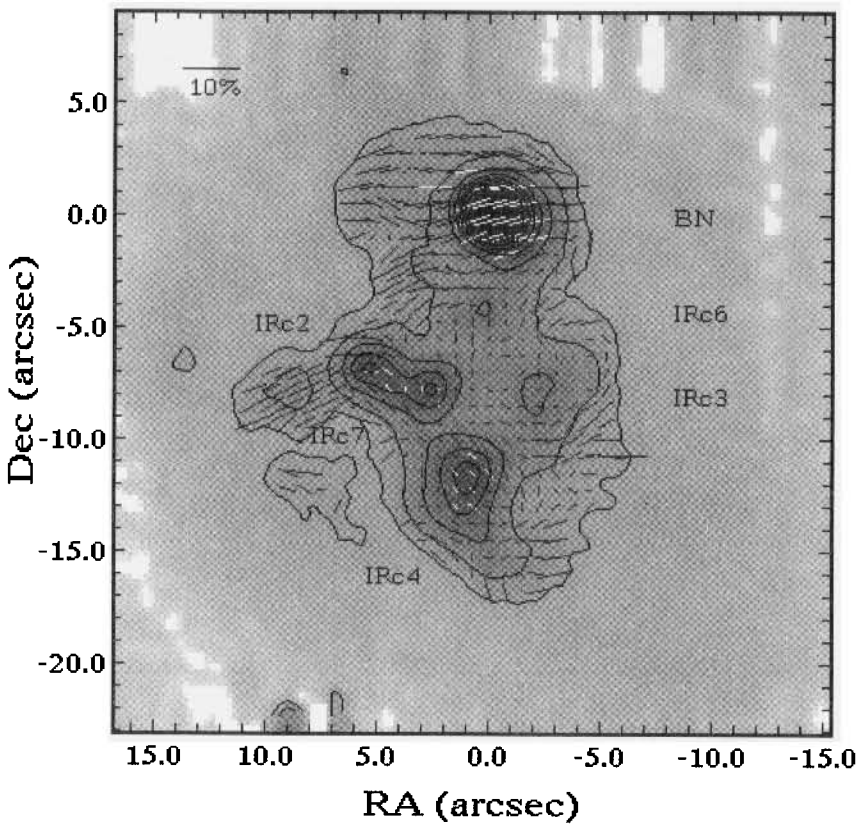

Figure 1. (a) 12.5-μm surface brightness and polarization in the BNKL region of Orion; coordinate offsets are from the BN object. The contour intervals are at 5 per cent of the BN peak and have been truncated at 25 per cent of the peak. The polarization data have been smoothed by a 1.5 arcsec FWHM Gaussian and the vectors presented every third row and column.

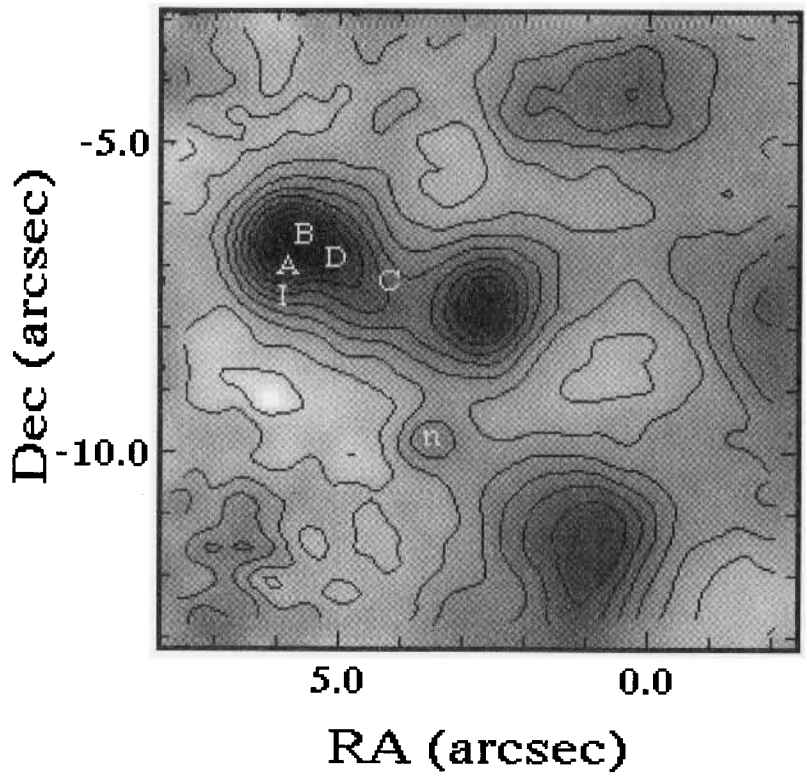

Figure 1. (b) Detail of the 12.5-μm surface brightness to show structure in the vicinity of Irc2 and Irc7. The original image has been smoothed by a 0.4 arcsec FWHM Gaussian and displayed after some unsharp masking to emphasize low-contrast detail. The sources 'A', 'B', 'C' and 'D' of Dougados et al. (1993) are indicated, as are the non-thermal radio sources 'I' and 'n' or 'L'.

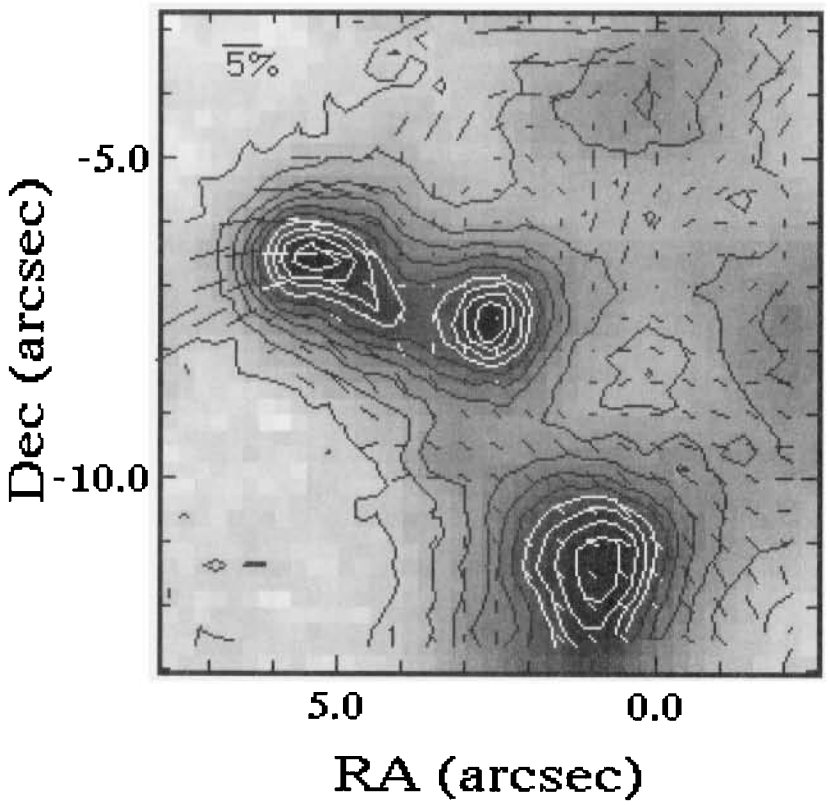

Figure 1. (c) 12.5-μm polarization vectors in the vicinity of Irc2 and Irc7: polarization vectors are plotted every second row and column.

the infrared source 'n' which is associated with the 22-GHz non-thermal radio source 'L' of Menten & Reid (1991). There is also a hint of the 3.8-μm source 'C' of Dougados et al. (1993) mid-way between Irc2 and Irc7, but these observations do not resolve the sources 'A', 'B' and 'D'. High-resolution observations by Menten & Reid (1995) at 8.4 and 43.1 GHz demonstrate that the radio continuum source 'I' does not coincide with any of the components of Irc2 but is coincident with the centroid of the SiO maser distribution. It appears that BN is the only infrared condensation coincident with a thermal radio source, and Menten & Reid (1995) and Gezari & Backman (1993) infer that Irc2 itself may not be internally heated and that there may be other sources of significant luminosity.

It is noticeable that the position of Irc4 at 12.5 μm is 1.5 arcsec south and east of Gezari & Backman's 8.7-μm position, but our position lies within the tail-like extension of the latter image in this direction; Gezari & Backman's longer wavelength images also show that effect. At 3.8 μm Dougados et al. (1993) resolve two sources corresponding to these positions, the brighter coinciding with the 8.7-μm source.

Fig. 1(c) shows the 12.5-μm polarization vectors in the region of Irc2 and Irc7. Dougados et al. (1993) present a high spatial resolution polarization image at 3.8 μm using a speckle technique; their polarizations are in the range 10–15 per cent, compared with $\lesssim 3$ per cent at 12.5 μm. Except in the vicinity of source 'n', the position angles agree tolerably well, but the polarization fractions are much larger in the 3.8-μm image and probably contain a large scattered component; in the 12.5-μm image the polarization at Irc7 is $\lesssim 0.5$ per cent and of the order of systematic errors.

Fig. 2(a) shows polarization vectors superimposed on the 17-μm intensity contours; the intensity has been smoothed with a 0.7 arcsec FWHM Gaussian, so that the spatial resolution here is essentially the diffraction limit of 1.1 arcsec at this wavelength; the polarization vectors are derived from images smoothed by 1.5 arcsec FWHM Gaussians and presented every third row and column.

In the 17-μm image (Fig. 2a) the contrast between the discrete sources and the diffuse material is much lower because of the increased surface brightness of the latter, and substantial polarization can be traced through much of the region. Corresponding large changes in polarization to those in Fig. 1(a) are seen.

At 17 μm the BN object appears elongated, with FWHM 2.9 arcsec at position angle $\simeq 35°$ and 2.3 arcsec orthogonal to this direction, roughly parallel to the polarization vectors. Both of these dimensions are significantly greater than the resolution which was about 2 arcsec diameter FWHM, and slightly larger than the diffraction limit due to seeing. The position of Irc4 is slightly displaced to the south-east from its position at 12.5 μm.

Fig. 2(b) shows detail of the 17-μm image in the region around Irc2 and Irc7, and generally shows a similar trend of position angle to that at 12.5 μm, although there is a noticeable difference in polarization fraction at Irc7. Here, and at the position of source 'n', the polarizations are roughly orthogonal to those of Dougados et al. (1993).

The most striking aspect of the polarization in Figs 1 and 2 is the strong variation of both position angle and polarization fraction throughout the region. Only around BN and the region north do the position angles correspond to the

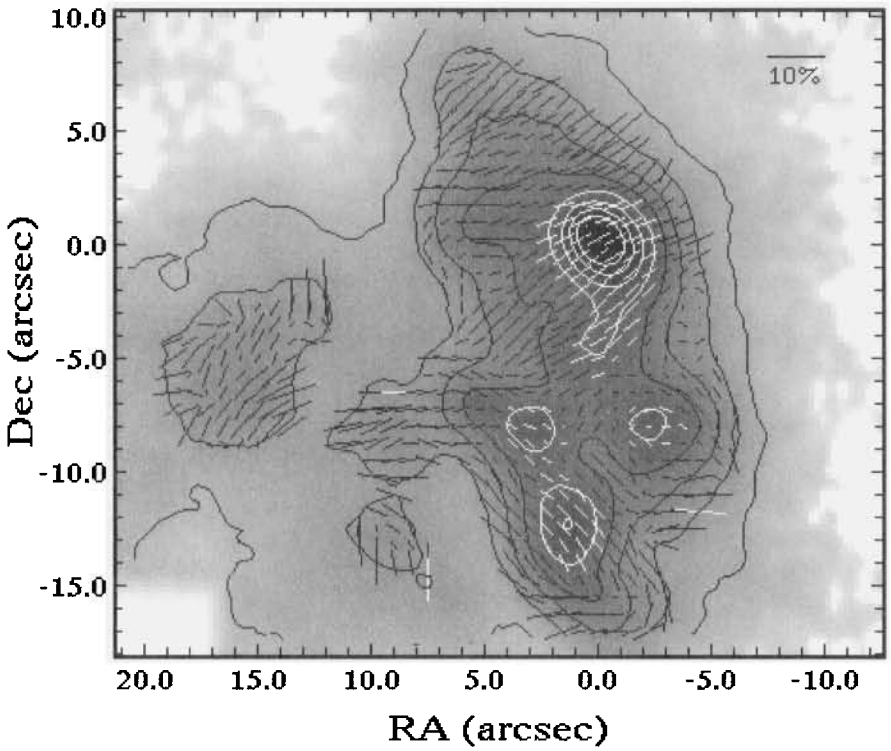

Figure 2. (a) The 17-μm surface brightness and polarization of BNKL. The contour intervals are at 7 per cent of the BN peak and truncated at 50 per cent of the peak; the polarization smoothing and sampling are as in Fig. 1(a).

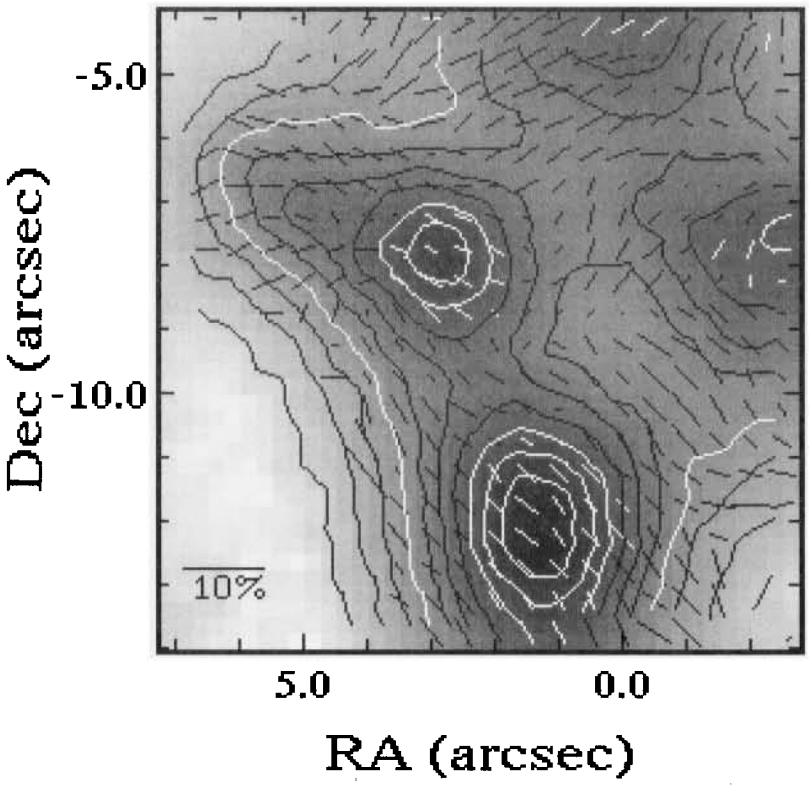

Figure 2. (b) Detail of the observed 17-μm polarization around Irc2 and Irc7.

almost uniform magnetic field observed in OMC-1 by Gonatas et al. (1990) and Hildebrand et al. (1995) at 100 μm; elsewhere there are very large shifts in position angle from the 'canonical' value of $\simeq 120°$ which pervades much of the northerly ridge of OMC-1.

3.1 The polarization mechanism

For the bright source BN, the polarization mechanism has been shown to be dichroic absorption by aligned grains, but elsewhere the polarization mechanism is not so clearly defined and must be established. We can rule out scattering on arguments over and above those appealing to the long wavelengths involved. First, the position angles in general bear no resemblance to those expected from scattering as observed in the near-infrared. Secondly, the polarized surface brightness everywhere increases between 12.5 and 17 μm, in particular at Irc4 from ~ 50 mJy arcsec^{-2} to ~ 1 Jy arcsec^{-2}; this effectively rules out a scattering mechanism.

What remains is dichroic absorption/emission by aligned grains. Since the orientation of the alignment direction will be determined by the ambient magnetic field irrespective of the mechanism that produces alignment, as was emphasized in the Introduction, we adopt the usual conclusion and take absorptive polarization to have the direction of the component of the magnetic field in the plane of the sky and emissive polarization to be orthogonal to the field.

It remains to determine whether or not the polarization is due to absorption uniformly throughout the image, and if not to establish the importance of the presence of any emissive components, as these would obviously affect the derivation of magnetic field directions. In particular, the position angles in and close to Irc4 are roughly orthogonal to those in and around the BN object, itself characteristic of the larger scale field direction. Before it can be established that there are field changes of this amount, the polarization around Irc4 must be demonstrated to be predominantly due to absorption rather than emission by aligned grains. Observations at a single wavelength cannot resolve this problem, but the spectral profiles of polarized emission, $p_{\rm em}(\lambda)$, polarized absorption, $p_{\rm abs}(\lambda)$, and extinction, $\tau(\lambda)$, are related by the expression

$$p_{\rm em}(\lambda) \simeq -p_{\rm abs}(\lambda)/\tau(\lambda)$$

to a good approximation (e.g. Hildebrand 1988; Aitken 1989). So long as $\tau(\lambda)$ is a strong function of λ, as it usually is in the 8–13 μm region and certainly in Orion, polarized emission and absorption will have different spectral profiles and can be readily distinguished.

Earlier spectropolarimetric observations between 8 and 13 μm (Aitken et al. 1985) established that the polarization of the BN object is due to absorption by aligned grains and that there is little, if any, contribution from an emissive polarization component. These observations also indicated that in Irc3, Irc4 and a position displaced from BN by 16 arcsec east and 6 arcsec south (SEBN) there was evidence for predominantly absorptive polarization, although contributions from other processes could not be ruled out. In Irc2 the spectral form of the polarization was more suggestive of polarized emission. The beamsize used in these observations (4.2-arcsec diameter) was such that in the latter case there would have been contamination from Irc7. In all of these sources the 8–13 μm polarization is much smaller than in BN, although the apparent extinction optical depth is much greater.

Further spectropolarimetric observations of the above sources and a number of other regions were obtained at the AAT and UKIRT in the wavelength ranges 8–13 and 16–22 μm. Some of these were with a smaller (2.6-arcsec diameter) beam, which allows better separation of Irc2 and Irc7. For a given grain shape and material, the polarization spectrum of the absorptive component is independent of optical depth, and of degree and angle of grain alignment. Provided that the emission is optically thin, the emissive polarization spectrum is independent of alignment and also grain temperature. Under these conditions, the two profiles are essentially invariant and the Stokes Q and U spectra can be independently fitted with the amplitudes of these two components. These procedures are further outlined by Aitken (1996), and are limited mainly by the quality of the data. Strictly these methods apply only to the separation of optically thin polarized emission from the absorptive polarization, both due to BN-like material. In the present case, a significant optical depth could be involved in any emission component present, but, since such polarized emission has a fairly muted spectral profile through the 8- to 13-μm region, the main effect of increasing optical depth would be to reduce the amount of emissive polarization rather than change significantly the spectral shape. A temperature distribution will not change the polarization spectrum. Some of these results are summarized in Table 1, and lead to the following comments on individual sources.

Table 1. 8–13 and 16–22 μm spectropolarimetry.

source	offsets[1] α	offsets[1] δ	8–13μm[2] 11–13μm p	11–13μm θ	abs.[3] p	abs.[3] θ	em.[3] p	em.[3] θ	16–22μm[2] p	16–22μm[2] θ
BN	0	0	11.3±.1	118±.2	12.6±.2	118±.5	-	-	9.1±.2	117±.5
Irc2	5.6	-7.0	3.6±.3	102±3	5.8±.7	123±4	3.5±.4	58±5	2.8±.4	113±4
Irc3	-2.2	-7.5	2.7±.4	94±5	6.8±1	87±5	3.6±.6	172±5	2.7±.2	90±2
Irc4	1.5	-12.0	2.5±.1	46±1	4.5±.3	44±2	1.6±.2	132±3.5	1.2±.1	50±1.5
Irc6	0.2	-3.5	5.3±.1.5	109±8	5.3±.9	96±5	-	-	6.3±.2	114±1
Irc7	2.8	-7.8	1.8±.2	94±3	3.9±.9	118±7	2.6±.5	42±6	1.4±.1	92±2.5

[1]Offsets are from BN in arcseconds. [2]Columns headed 8–13 and 16–22 μm are observed averages within the range. [3]Columns 'abs.' and 'em.' are separated components at 10 and 12 μm respectively (see text). p and θ are in per cent and degrees (north through east) respectively.

Irc4. There is a component of polarized emission with about one-third the amplitude (at $\simeq 12$ μm) of the absorptive polarization (at $\simeq 10$ μm) and orthogonal to within the uncertainties of a few degrees. This hardly affects the observed position angle, but reduces the polarization observed to two-thirds of the absorptive value. The implied magnetic field projected direction of $\simeq 42°$ in the emitting region is essentially the same as in the (presumed) overlying absorptive region. Fig. 3(a) shows the 8–22 μm spectropolarimetry of Irc4. The apparent discontinuities in polarization between 18 and 20 μm are almost certainly of statistical origin.

Irc3. Here an emissive component has about half the polarization of the absorptive component and is again orthogonal within the errors. Thus the observed polarization is about half that of the absorptive component, and the magnetic field directions in the emitting and absorptive regions are similar and at a position angle of $\simeq 90°$.

Icr7. The emissive component is about two-thirds of the absorptive component and the two position angles differ from orthogonality by $\simeq 15°$; the observed polarization in the 10-μm region here is small and the consequent signal-to-noise ratio in the separated components poor, so that here again the field direction may not significantly differ from the observed position angle of $\sim 95°$ at 10 μm.

Irc2. The emissive component is rather more than half the absorptive component; the former has a position angle of $\simeq 58°$ and the latter $\simeq 123°$. The overlying field direction of $\simeq 123°$ is significantly different from the observed polarization of 90°–100°, and the field in the emissive region has a position angle of $\simeq 150°$. Irc2 has the deepest extinction feature in this region with an optical depth $\tau_{10\,\mu m} \simeq 8$ corresponding to $A_V \sim 150$ mag. [Note that the 10-μm optical depths quoted here (Aitken et al. 1981) differ from those in Gezari & Backman (1993) because we have included the effects of the underlying silicate emission in some of the sources.]

A somewhat surprising result is that, even when a significant 8–13 μm emission component is present, the 16–22 μm position angle is still more strongly representative of absorption. It seems likely that at 16–22 μm there is less sensitivity to local warm dust in the vicinity of the discrete sources, and there is dilution by emission from a cooler diffuse background.

In the more diffuse regions of low surface brightness, 8–13 μm spectropolarimetry cannot meaningfully separate the components. In some cases, however, the 16–22 μm spectropolarimetry shows a polarization peak and a weak absorption feature, both similar to those seen in BN, such as in Irc6 shown in Fig. 3(b), so that absorptive polarization probably extends over the region.

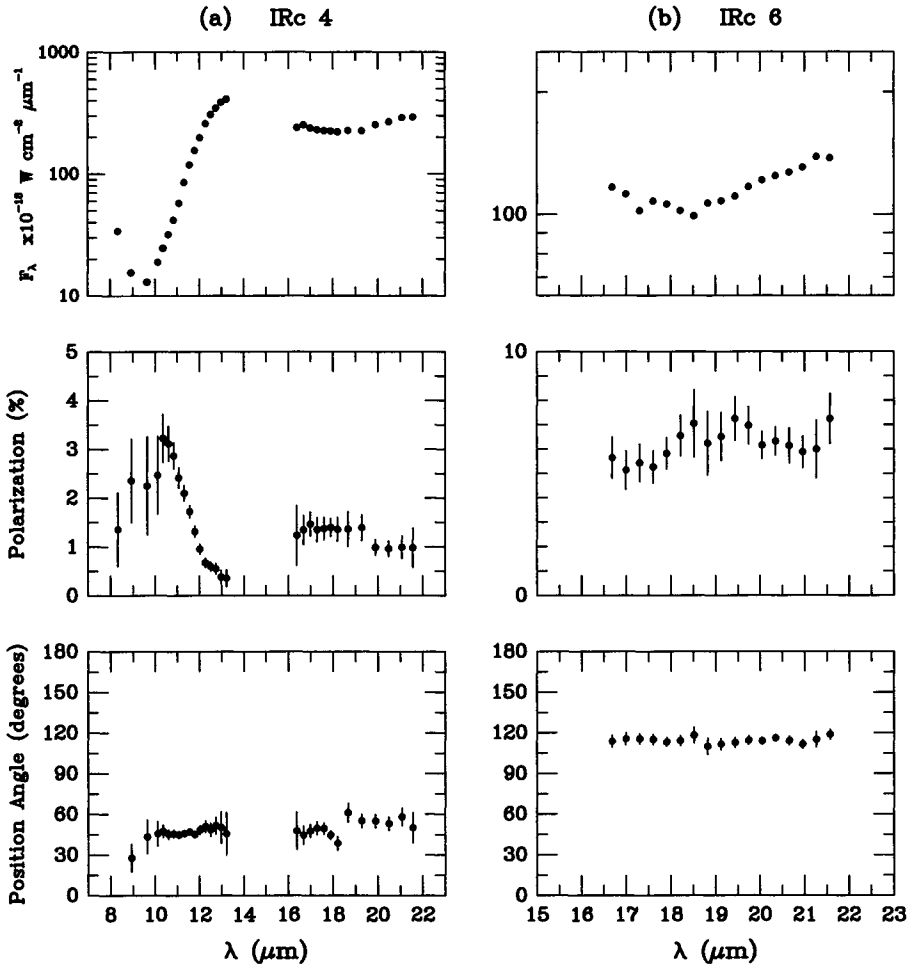

Figure 3. (a) The 8–22 μm spectropolarimetry of Irc4. (b) The 16–22 μm spectropolarimetry of Irc6.

It thus appears that, although some of the discrete sources in BNKL do have an emissive component, this only significantly affects the determination of magnetic field direction in Irc2. The field direction in the warm inner region of Irc2 seems to be increased by $\sim 30°$ (north through east) with respect to the overlying cold material in which the line-of-sight averaged field direction is close to the 'canonical' value of 120°.

3.2 Comparison with results at other wavelengths

3.2.1 Far-infrared

Studies by Gonatas et al. (1990) and Hildebrand et al. (1995) at 100 μm have established the presence of a large-scale, predominantly undirectional magnetic field normal to the long axis of the Orion molecular cloud; similar results have been obtained at 1300 μm by Leach et al. (1991), at 800 μm (this work) and at 450 μm by Schleuning, Dowell & Platt (1996). The 800-μm results are shown in Fig. 4 superimposed on the 450-μm contours of Wright et al. (1992). Except near the central intensity peak, the region covered in the present work, all of these data show polarization in the range 4–7 per cent with position angles close to 30°; near the peak the polarization falls to 1–2 per cent without appreciable change of position angle. The far-infrared results have effective beamsizes of 40 ($\lambda = 100$ μm), 16 ($\lambda = 450$ μm), 14 ($\lambda = 800$ μm) and 30 ($\lambda = 1300$ μm) arcsec, which are all more than an order of magnitude larger than for the mid-infrared work presented here, and they all probe essentially the whole depth of OMC-1 and are biased to cooler grains.

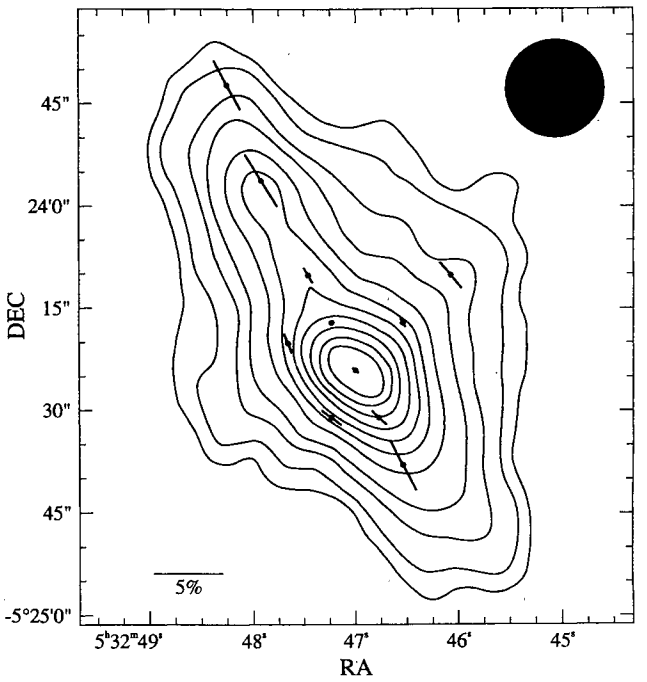

Figure 4. 800-μm polarization superposed on the 450-μm surface brightness contours of Wright et al. (1992). Contours are at 2.5, 5, 10, 15, 20, 30, 40, 50, 60, 70 and 80 per cent of the peak flux density of 375 Jy beam^{-1} (0.041 K Jy^{-1}).

Gonatas et al. (1990) estimate the emissivity at 100 μm to be between 0.2 and 0.3, so that the reduction in polarization due to self-absorption would be less than 20 per cent; a substantial optical depth due to similarly aligned overlying cold dust would also reduce the observed polarization. The similarity of the far-infrared results over a wavelength range from 100 to 1300 μm argues that the same grain population is being sampled through the entire depth of the cloud, amounting to $A_V \sim 500$ mag for a hydrogen column density of 10^{24} cm^{-2} (Genzel & Stutzki 1989, and references therein).

At 10 μm the apparent optical depth varies from 3.3 mag towards BN to $\simeq 8$ mag towards Irc2; spectropolarimetry suggests that in the diffuse regions it lies between these two values. The corresponding range of optical extinction is $60 < A_V < 150$ mag at 10 μm. At 17 μm the extinction is less and in the diffuse regions we may be sampling deeper, to perhaps half-way through the cloud.

By applying software-defined apertures to the 17-μm data, we have reproduced the effect of observations using apertures approaching those used in the far-infrared work, and centred on the far-infrared observations close to the peak intensity. These are compared in Table 2, where it is seen that the 100- and 1300-μm position angles are orthogonal to within 10° to those in 17-μm equivalent apertures. The discrepancies are much greater for the 450- and 800-μm positions and beamsizes but may be due, at least in part, to the increasing indeterminacy of position angle at low measured polarization. Considering also that the 17-μm large-

Table 2. Comparison with far-infrared and submillimetre observations.

	Far-infrared/sub-mm					17μm		
λ	offset†		beam	p	θ	beam	p	θ-90
(μm)	α	δ	(arcsec)	(%)	(degrees)	(arcsec)	(%)	(degrees)
100(1)	3	-2.5	40	1.8	16	20	2.0	26
450(2)	4.5	-7.5	16	1	40	16	1.0	8
800(3)	-0.5	-2.0	14	0.7	52	14	2.0	29
1300(4)	1	-0.5	30	2.7	34	20	2.8	29
1300(4)	0	0				1	6.2	28
1300(4)	3.5	-4				36×28	1.5	111‡

†Offsets in arcseconds from BN. ‡Whole image space.
(1) Gonatas et al. (1990). (2) Schleuning et al. (1996). (3) This work. (4) Leach et al. (1991).
Statistical errors on the 17-μm data: 0.1–0.2 per cent and 1°–5°.

aperture results do not penetrate as deeply into the source as do those in the far-infrared, we conclude that the low polarization observed very close to the peak is consistent with being due solely to field complexity in this region.

In the 12.5-μm image the contrast between BN and both the diffuse background and the other compact sources is so much greater than at 17 μm that even in the whole frame the polarization is dominated by BN.

3.2.2 Near-infrared

Observations over the central arcminute at comparable resolutions in the 2.12-μm S(1) emission line of molecular hydrogen have been presented by Chrysostomou et al. (1994); in this central region the line polarization is attributed to dichroic absorption. There is general consistency with the present work in regard to the comparison of position angles, except in and near to Irc4 where the polarizations are roughly orthogonal. Also, near the Irc2 and Irc7 association, the 17-μm position angles are significantly smaller than in the hydrogen line (that is, they appear to be more twisted in the mid-infrared). There are marked differences in the variation of polarization fraction across the images: in the long-wavelength image this tends to be more uniform, while in the line image the polarization becomes much smaller in the north-east–south-west association of Irc4, Irc7 and Irc2, and extends further north-east. It seems likely that sampling of greater depths along the line of sight in the 17-μm image can explain these effects.

Dougados et al. (1993) present a speckle polarimetric image at 3.8 μm of the vicinity of Irc2, in which region the position angles are similar to those in Fig. 2; at Irc7, however, the corresponding position angles are approximately orthogonal. Minchin et al. (1991) also present continuum imaging polarimetry from 1.25 to 3.6 μm, but in substantial areas away from BN their position angles differ significantly from those in this work, although a change in magnetic field direction near Irc2 is indicated. Most of these differences can be attributed to a scattering component in the shorter wavelength continuum data.

3.3 The third dimension and the central field configuration

The large-scale field in OMC-1, as revealed by the far-infrared observations, is, to first order, uniform with position angle $\simeq 120°$, normal to the elongation of the north-north-east ridge of dust and gas, and it seems that collapse along the field direction could have produced the elongated structure. The far-infrared polarizations are typically 5–7 per cent, except close to the intensity peak where the polarization falls to a minimum value of $\simeq 1$ per cent. The position of low polarization corresponds approximately to the central ~ 10 arcsec around Irc2 where the mid-infrared changes of polarization are large and complex, and at the least imply dynamical activity in this region.

Chrysostomou et al. (1994) have compared their derivation of the field structure with the specific model of a rotating disc located close to Irc2 in which an initial poloidal magnetic field becomes twisted by differential rotation (Newman, Newman & Lovelace 1992). They obtain some qualitative agreement with the model and conclude that such a poloidal disc field is not inconsistent with the field twisting around the position of Irc2 that they observe.

Although the present data differ in significant respects from the S(1) line image, they too are probably in a general way consistent with the Newman et al. (1992) configuration in that there is a component of field with position angle $\simeq 65°$, roughly orthogonal to the large-scale field and corresponding to the line joining the Irc2 complex of sources with Irc7 and the presumed disc plane. Even so, it is not clear that the model of Newman et al. (1992), starting from a disc with an initially poloidal field, is appropriate to describe the situation in OMC-1 where the inner disc field presumably develops during collapse from a pre-existing field. It may be that the end result is similar: a toroidal disc field component merging into the larger scale field directed along the CO flow. Rather than pursue this comparison further, however, we will investigate these polarimetric data in relation to the complex structures in the vicinity of Irc2 revealed by millimetre-wave studies (Plambeck et al. 1982; Erikson et al. 1982; Masson & Mundy 1988; the review of Genzel & Stutzki 1989, and references therein; Murata et al. 1991).

The picture that emerges from these studies is of a dense disc-like slab of dust and molecular gas with symmetry axis $\simeq 300°$–$310°$ coinciding with the blueshifted CO flow (Erikson et al. 1982), and the centre of which is close to Irc2. This slab is inclined away from us towards the north-west and, with an optical depth $\tau_{20\,\mu m} \sim 10$–30 (Plambeck et al. 1982), is the limiting visible surface at all near and mid-infrared wavelengths. The regions of low surface brightness in BNKL, away from the discrete sources, have 16-μm/22-μm colour temperatures in the range 100–120 K and brightness temperatures of 80–90 K; this suggests that most of the diffuse continuum emission arises from material in front, or at the near face of this slab. Wright et al. (1992), from observations at 3.5 mm and 450 μm, find dust temperatures of 100–200 K for the 'hot core' region, but their beam would include Irc2.

Spectroscopy at 8–13 μm, and to a lesser extent 16–22 μm, gives a guide to the extinction to the discrete sources. BN has been estimated to have $\tau_{9.7\,\mu m} \simeq 3.3$ after allowance for a local emission component, whereas for Irc2 and Irc4 the corresponding values are 7.9 and 5.7 respectively (Aitken et al. 1981); the extinction towards Irc2 is the largest measured in BNKL, and the intervening diffuse regions appear to have extinctions in the range $\tau_{9.7\,\mu m} \sim 3$–5. In terms of the preceding discussion Irc2, and possibly Irc4, is partially embedded within the tilted disc and the intervening medium, which includes the outflow and related phenomena, provides the extinction and polarization to the outlying regions of BNKL.

Fig. 5 shows the 17-μm polarization fraction image. Because polarization is a positive definite quantity, it is subject to positive bias at low signal-to-noise ratio, and for this reason the lower flux regions are excluded from this image which has been smoothed with a 2.5 arcsec FWHM Gaussian. It is noticeable that there is little association between the discrete sources BN, Irc2, Irc3, Irc4 and Irc7 and the polarization contours, this is shown more clearly in Fig. 6 in which cuts through BN in intensity and polarization fraction are shown after the same smoothing. An extended region near BN is a polarization maximum, indicating that the intervening material is similarly polarizing BN and the

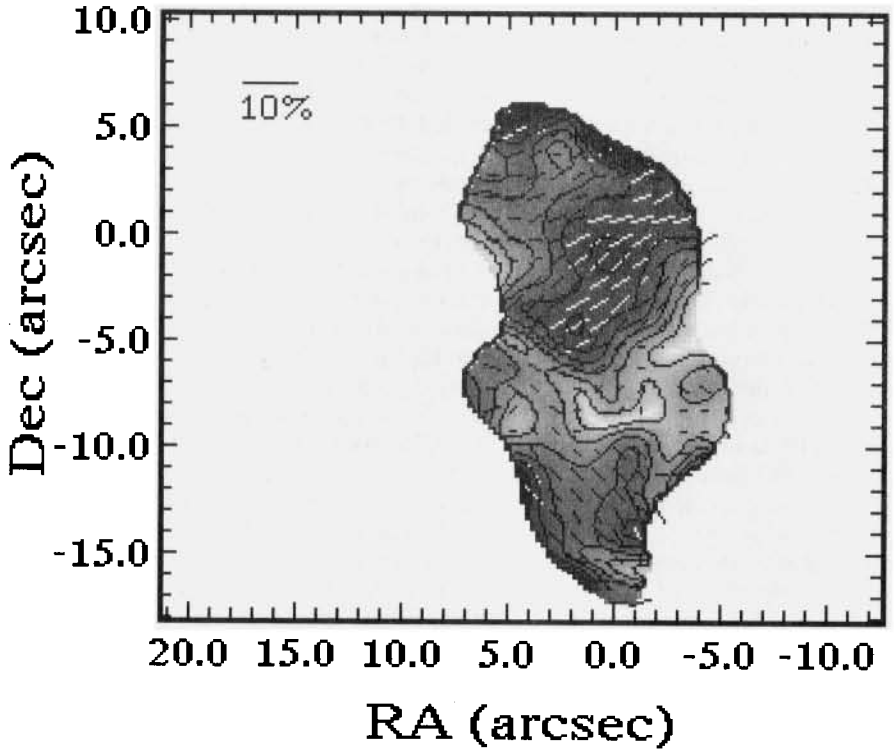

Figure 5. Contours of 17-μm polarization fraction. The polarization data have been smoothed with a 2.5 arcsec FWHM Gaussian to reduce errors due to positive bias.

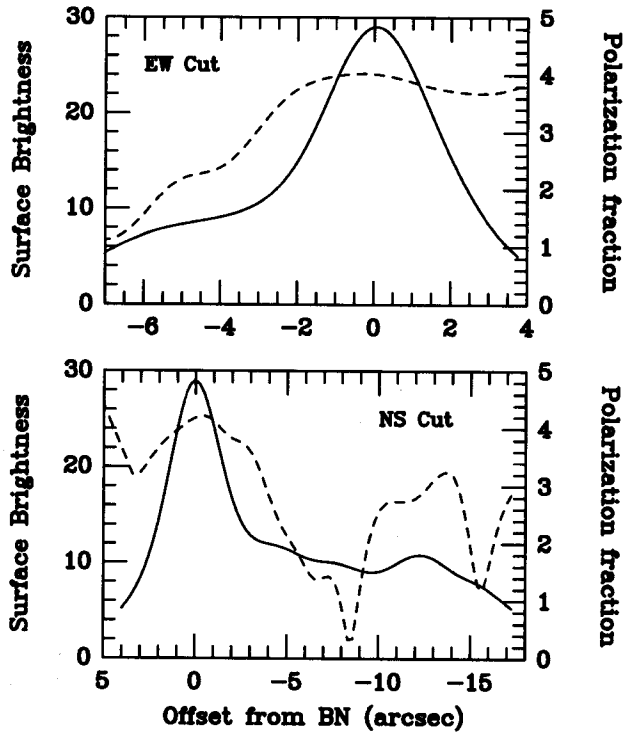

Figure 6. Cuts through BN of 17-μm surface brightness (solid lines) and polarization fraction (broken lines); both quantities have been similarly smoothed as in Fig. 5. Axial tick marks are at arcsecond intervals.

diffuse emission. That BN itself does not introduce dilution of polarization suggests that it is at the far edge of the polarizing medium. The other characteristic of Fig. 5 worthy of comment is that there appear to be two distinct regions of polarization separated by a line of low polarization running roughly south-east and about 2 arcsec north of an Irc2–Irc7–Irc4 axis. The two regions have different orientations: the northern region has position angles predominantly near 120° but extending from 90 to 130° compared with 30° to 90° in the southern region, with a dominant component near 45°.

The S(1) H_2 emission is polarized at the 4–7 per cent level, compared with the adjacent *K*-band continuum polarization of 18 per cent towards BN (Burton et al. 1991; Chrysostomou et al. 1994). Since the polarization of BN is produced by the overlying medium, and is not peculiar to BN, the implication must be that the H_2 polarization samples the medium closer to us than does BN. The simplest case to consider is where the H_2 emission comes from a region in which grains are either absent or not aligned, and then the observed line polarization of 5.5 per cent must arise in overlying material with a further 12.5 per cent polarization to the BN object lying beyond the H_2 region. On the other hand, if the H_2 emission is distributed along part of the line of sight within the dichroic medium, the polarization will be reduced due to self-dilution. If the region within which the H_2 is distributed produces polarization p_0 per unit optical depth, the observed H_2 polarization will be

$$p_{H_2}=p_0\frac{1-e^{-\tau_2}(\tau_2+1)}{1-e^{-\tau_2}}=p_2\frac{1-e^{-\tau_2}(\tau_2+1)}{\tau_2(1-e^{-\tau_2})},$$

where τ_2 is the extinction and p_2 is the observed polarization of an unpolarized background source. For small τ_2 then $p_{H_2}\rightarrow p_2/2$ and, for large τ_2, $p_{H_2}\rightarrow p_2/\tau$, the specific polarization of the medium in which the H_2 emission is embedded (essentially the H_2 polarization samples only to an optical depth of unity). p/τ is typically in the range 1–2 per cent for continuum polarization, and it follows that a large part of the observed value of $p_{H_2}\simeq 5.5$ per cent must arise in the overlying material, while the line polarization probes only the succeeding unit optical depth. Thus in the present case the H_2 polarization is representative only of the near third or so of the line-of-sight polarization to BN.

Because the disc is inclined to our line of sight, we envisage that the intervening polarizing material is in the form of a wedge. This is similar to the suggestion of Hough et al. (1986), who invoked an inclined dichroic sheet of material in front of BNKL to describe the H_2 and *K*-band polarization. Here, however, the depth of dichroic material associated with the polarization increases along a direction normal to the disc plane, also the direction of the ambient field, with position angle $\simeq 300°$. The other parameters of this wedge are harder to judge: it presumably would produce little polarization south-east of the Irc2–Irc7–Irc4 axis where the wedge is thin and the disc is the limit of visibility. At the distance within the wedge typical of BN, the polarization due to the wedge will be large and as a first guess that of the BN object at 17 μm. On this picture the vicinity of Irc4 suffers only small polarization from the wedge, and most of the observed polarization is ascribed to absorptive polarization arising within the disc and representative of a field within the disc. Elsewhere the observed polarization is the result of the summation of a disc field with the effect of the dichroic wedge. The effect of removing the polarization produced by such a wedge, with gradient direction 300° such that at and south of Irc2 it is zero, north of BN it is 5.5 per cent at position angle 120° and has a linear gradient between, is shown in Fig. 7. As expected, the field directions are now more uniformly directed normal to the symmetry axis of the disc, but new variations of position angle are also introduced. The wedge that we have introduced is idealized. More realistically, it contains an outflow region of uncertain geometry in which grain properties and alignment may differ from those in more quiescent material, and with enough free parameters to make further modelling increasingly arbitrary. It should be remembered that absorptive polarization gives the averaged polarization along the line of sight and, from the shift in position angle between ice feature and continuum polarization towards the BN object (Hough et al. 1995), there is clear evidence for twisting of the alignment direction by $\sim 30°$ along this line of sight.

There have been violent and energetic events in Orion, as revealed by the dramatic results of Allen & Burton (1993). The origin of these events appears to have been the BNKL complex some 10^3 or so years ago, and it is hard to know to what extent such events have left their mark in disturbing and stirring the region. Even so, and without any appeal to modelling, the substantial absorptive polarization lying near or in and parallel to the disc plane is strong evidence for the presence of a toroidal field within this structure.

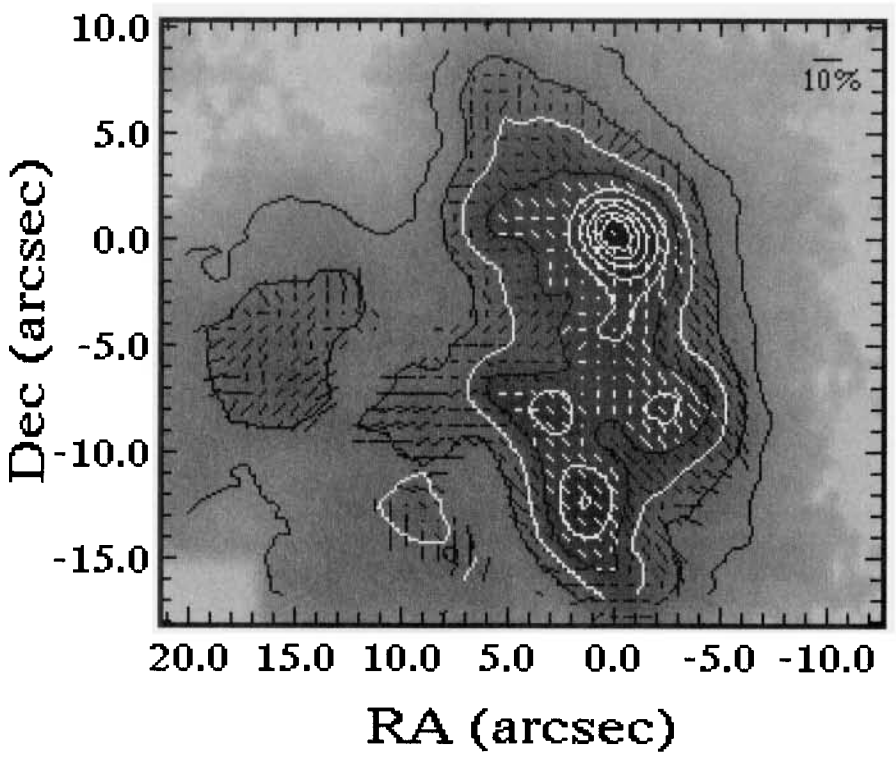

Figure 7. 17-μm polarization image after correction for the effects of a dichroic wedge (see Section 3.3 for details).

4 CONCLUSIONS

Polarimetric observations of Orion at 800 μm with 14-arcsec resolution show similar behaviour to that seen at other far-infrared wavelengths, namely polarizations largely aligned with the elongation of OMC-1 and indicating a magnetic field normal to this ridge, but with greatly reduced polarization within the central half arcminute.

Polarimetric imaging of this central region at 12.5 and 17 μm with arcsecond resolution shows substantial changes of polarization and position angle on the scale of several arcseconds. These variations can explain the reduced far-infrared polarization observed with beams that do not resolve this structure; there is no need to invoke changes of grain chemistry, geometry or alignment efficiency in this region.

Spectropolarimetry in the ranges 8–13 and 16–22 μm shows that the mid-infrared polarization is predominantly due to dichroic absorption by aligned grains. The 17-μm images thus show that, in addition to a magnetic field direction with position angle $\simeq 120°$ indicated by the far-infrared studies, there is a substantial central component south-west of Irc2 with a nearly orthogonal field. A likely interpretation of this is the presence of a toroidal field component lying in the plane of the disc-like structures which have been observed in millimetre-wave studies.

ACKNOWLEDGMENTS

We are pleased to acknowledge useful discussions with Roger Hildebrand, and thank him and David Schleuning for access to material prior to publication. DKA acknowledges with thanks the support of a Leverhulme Trust Grant, a Visiting Professorship with University College, ADFA, and the use of facilities at the University of York and Royal Observatory Edinburgh. CHS is supported by an Australian Research Council Senior Research Fellowship. We would also like to thank PATT and ATAC for the award of observing time, and also the staff of UKIRT and the AAT for their cheerful assistance.

REFERENCES

Aitken D. K., 1989, in Kaldiech B. H., ed., Proc. 22nd ESLAB Symp. on Infrared Spectroscopy in Astronomy. ESA Publ., SP-290, p. 99
Aitken D. K., 1996, in Roberge W., Whittet D. C. B., eds, ASP Conf. Ser. 97, Polarimetry of the Interstellar Medium. Astron. Soc. Pac., San Francisco, p. 225
Aitken D. K., Roche P. F., Spenser P. M., Jones B., 1981, MNRAS, 195, 921
Aitken D. K., Bailey A. J., Roche P. F., Hough J. H., 1985, MNRAS, 215, 425
Allen D. A., Burton M. G., 1993, Nat, 363, 54
Burton M. G., Minchin N. R., Hough J. H., Aspin C., Axon D. J., Bailey J. A., 1991, ApJ, 375, 611
Chrysostomou A., Hough J. H., Burton M. G., Tamura M., 1994, MNRAS, 268, 325
Dolginov A. Z., Mytrophanov L. G., 1976, Ap&SS, 43, 291
Dougados C., Lena P., Ridgway S. T., Christou J. C., Probst R. G., 1993, ApJ, 406, 112
Dyck H. M., Lonsdale C. J., 1981, in Wynn-Williams G. C., Cruikshank D. P., eds, Proc. IAU Symp. 96, Infrared Astronomy. Reidel, Dordrecht, p. 223
Dyck H. M., Cappa R. W., Forrest W. J., Gillett F. C., 1973, ApJ, 183, L99
Erikson N. R., Goldsmith P. F., Snell R. L., Berson R. L., Huguenin G. R., Ulrich B. L., Lada C. J., 1982, ApJ, 261, L103
Genzel R., Stutzki J., 1989, ARA&A, 27, 41
Gezari D. Y., Backman D. A., 1993, in McLean I., ed., Astronomy with Infrared Arrays – The Next Generation. Kluwer, Dordrecht, p. 195
Gonatas D. P. et al., 1990, ApJ, 357, 132
Harwit M., 1970, Nat, 226, 61
Hildebrand R. H., 1988, QJRAS, 29, 327
Hildebrand R. H., Dotson J. L., Dowell C. D., Platt S. R., Schleuning D., Davidson J. A., Novak G., 1995, in Haas M. R., Davidson J. A., Erickson E. F., eds, ASP Conf. Ser. Vol. 75, Airborne Astronomy Symposium on the Galactic Ecosystem. Astron. Soc. Pac., San Francisco, p. 97
Hough J. H. et al., 1986, MNRAS, 222, 629
Hough J. H., Chrysostomou A., Messinger D. W., Whittet D. C. B., Aitken D. K., Roche P. F., 1995, ApJ, 461, 902
Lazarian A., 1994, MNRAS, 268, 713
Leach R. W., Clemens D. P., Kane B. D., Barvainis R., 1991, ApJ, 370, 257
Martin P. G., 1975, ApJ, 202, 393
Masson C. R., Mundy L. G., 1988, ApJ, 324, 538
Masson C. R., Claussen M. J., Lo K. Y., Moffet A. T., Phillips T. G., Sargent A. I., Scott S. L., Scoville N. Z., 1985, ApJ, 295, L47
Menten K. M., Reid M. J., 1991, BAAS, 22, No. 4, 1269 (abstract)
Menten K. M., Reid M. J., 1995, ApJ, 445, L157
Minchin N. R. et al., 1991, MNRAS, 248, 715
Murata Y., Kawabe R., Ishiguro M., Hazegawa T., Hayashi M., 1991, in Falgarone E., Boulanger F., Duvert G., eds, Proc. IAU Symp. 147, Fragmentation of Molecular Clouds and Star Formation. Kluwer, Dordrecht, p. 357
Newman W. I., Newman A. L., Lovelace R. V. E., 1992, ApJ, 392, 622
Plambeck R. L., Wright M. C. H., Welch W. J., Bieging J. H., Baud B., Ho P. T. P., Vogel S. N., 1982, ApJ, 259, 617
Schleung D. A., Dowell C. D., Platt S. R., 1996, in Roberge W., Whittet D. C. B., eds, ASP Conf. Ser. 97, Polarimetry of the Interstellar Medium. Astron. Soc. Pac., San Francisco, p. 285
Smith C. H., Aitken D. K., Moore T. J. T., 1994, in Crawford D. L., Craine E. R., eds, Proc. SPIE 2198, Instrumentation in Astronomy III. SPIE, Bellingham, p. 736
Wright M., Sandell G., Wilner D. L., Plambeck R. L., 1992, ApJ, 393, 225